University of Rochester Report # UR 457

University of Michigan Report # UMBC 73-20

Production of γ, Λ°, K_S° and $\bar{\Lambda}^\circ$ in pp Collisions at 102 GeV/c.*

by

J. W. CHAPMAN, J. COOPER, N. GREEN, B. P. ROE, A. A. SEIDL and

J. C. VANDER VELDE

University of Michigan
Ann Arbor, Michigan

and

C. M. BROMBERG, D. COHEN#, T. FERBEL+, P. SLATTERY

University of Rochester
Rochester, New York

We have measured cross sections for γ, K_S°, Λ and $\bar{\Lambda}$ production at 102 GeV/c and find: $\sigma(\gamma) = 170 \pm 16$ mb., $\sigma(K_S^\circ) = 4.6 \pm 0.5$ mb., $\sigma(\Lambda) = 3.2 \pm 0.4$ mb., and $\sigma(\bar{\Lambda}) = 0.23 \pm 0.10$ mb.. Both $\langle n_{\pi^\circ} \rangle$ and $\langle n_{K_S^\circ} \rangle$ appear to rise linearly with n_- while the ratio $\langle n_{K_S^\circ} \rangle / \langle n_{\pi^\circ} \rangle$ is approximately independent of n_-. The integrated invariant cross section as a function of x as well as $d\sigma/dy$ and $d\sigma/dp_T^2$ are presented and compared with other data.

*Research supported by the U. S. Atomic Energy Commission
#Presently at Nevis Laboratories, Columbia University, Irvington, N. Y.
+A. P. Sloan Fellow

Using a 30,000 picture exposure of the 30-inch liquid hydrogen bubble chamber at the National Accelerator Laboratory to 102 GeV/c protons we have measured the inclusive production of γ, K°_s, Λ and $\bar{\Lambda}$. In order to find all events with an associated V° (K°_s, Λ or $\bar{\Lambda}$) or γ, two independent scans of the film were made and all conflicts between the two scans were resolved. Within a restricted fiducial volume a total of 505 V°/γ's were found to be associated with beam track interactions and 488 of these events were successfully measured.[1] These events were geometrically reconstructed and kinematically fitted using the TVGP-SQUAW program. A requirement that the mass of the e^+e^- pair be less than 20 MeV/c^2 was used to select γ candidates. The K°/Λ ($\bar{\Lambda}$) ambiguities were resolved through ionization information when possible or through a selection on the decay angle of the π^- with respect to the line of flight of the K°_s in the K°_s rest frame.[2] In addition all neutral particles were restricted to be in the backward hemisphere in the pp c.m. system. After all acceptance criteria were imposed there remained 124 γ's, 105 K°_s's, 76 Λ's, and 6 $\bar{\Lambda}$'s with average weights (inverse detection efficiencies) of 76.6, 2.39, 2.70 and 3.4 respectively.[3]

In Table I we list the inclusive cross sections and the average number of particles observed per inelastic pp interaction as a function of charged multiplicity for π°, K°_s and Λ production. We have assumed that all γ's come from π° decay and that $\sigma(\pi^\circ) = 1/2\ \sigma(\gamma)$. These total inclusive cross sections are in general agreement with the trends reported in other high energy pp experiments[4], and lend support to the observation that the Λ production cross section changes very slowly between 69 and

303 GeV/c.

In Figure 1 we plot the average number of neutrals observed per inelastic pp interaction as a function of charged topology. The ratio $\sigma(K_s^\circ)/\sigma(\pi^\circ) \sim 0.05$ is approximately independent of the associated charged multiplicity. The approximate linear rise of $\langle n_{\pi^\circ} \rangle$ is observed in all experiments at or above 69 GeV/c, in contrast to lower energy pp data[5] where $\langle n_{\pi^\circ} \rangle$ is approximately constant as a function of n_c. The dashed curve in Figure 1b is given by $\langle n_{\pi^\circ} \rangle = n_-$, a form to which high energy data has been compared. A better parameterization of the data at 102 GeV/c is $\langle n_{\pi^\circ} \rangle = (1.8 \pm 0.5) + (0.31 \pm 0.17)\, n_-$ (solid curve). The rise of $\langle n_{\pi^\circ} \rangle$ with n_- is not in agreement with the predictions of multiperipheral models in which single pions are independently emitted.[6] The total π° production cross section at 102 GeV/c, $\sigma(\pi^\circ) = 85 \pm 8$ mb., is comparable to the total π^- production cross section, $\sigma(\pi^-) = 66.9 \pm 1.3$ mb..

In Figure 2 we plot the invariant cross section integrated over p_T^2.

$$F(x) = \frac{2}{\pi\sqrt{s}} \int E \frac{d^2\sigma}{dx dp_T^2} dp_T^2$$

for γ, K_s° and Λ production. The curve in Figure 2a is an integral over p_T^2 of an interpolation formula suggested by Neuhofer et al[7] as a possible parameterization of γ production data at equivalent lab momenta of 500 GeV/c, 1100 GeV/c, and 1500 GeV/c. The small systematic difference observed in the applicable range of the formula (solid line) may indicate that the invariant cross section for γ production does not scale in this x region.

The invariant cross section for K_s° production, displayed in

Figure 2b, shows an exponential fall off, typical of meson distributions, with a slope of 4.7 ± 2.0 (solid curve). This slope is compatible with that observed at 205 GeV/c and 303 GeV/c. The data on F(x) for Λ production is similar in all experiments above 69 GeV/c, however, when compared to the 24 GeV/c data of Muck et al[8] (dashed curve) a rise is seen in the proton fragmentation region ($-x \gtrsim 0.6$).

In Figure 3 we plot $d\sigma/dy$ as a function of y (c.m. rapidity) for the above three reactions. Both γ and K_s° production are characterized by a plateau whose half width is approximately one unit in y. Distributions in transverse momentum are shown in Figure 4 where we plot $d\sigma/dp_T^2$ as a function of p_T^2. A typical rapid fall off is observed for all particle production with the steepness being a function of the mass of the produced particle.

In Table II we summarize the parameters of the p_T spectra for γ, K_s°, Λ and π^- production at 102 GeV/c.

We thank the staff of the 30-inch bubble chamber and the physicists from the National Accelerator Neutrino Lab for their considerable aid in obtaining this exposure.

REFERENCES

1. All cross sections have been corrected for unmeasurable events.
2. All events ambiguous between K^0_s and $\Lambda(\bar{\Lambda})$ interpretations were taken as $\Lambda(\bar{\Lambda})$ events if the cosine of the angle between the π^- and the direction of the K^0_s, measured in the K^0_s rest frame, was in the interval $-0.94 \leq \cos\theta \leq -0.86$ ($0.88 \leq \cos\theta \leq 0.92$). This selection introduces essentially no bias into the experimental spectra.
3. These weights do not include the additional factor of 2 required to correct for events produced in the forward hemisphere in the pp c.m. but they do include V° neutral branching values.
4. G. Charlton et al., Phys. Rev. Letters 29, 1759 (1972); G. Charlton et al., Phys. Rev. Letters 30 574 (1973); F. T. Dao et al., Phys. Rev. Letters 30 1151 (1973); France-Soviet Union Collaboration, "Photon Production in 69 GeV pp Interactions", paper submitted at Conference on New Results from Experiments on High Energy Particle Collisions, Nashville (1973); France-Soviet Union Collaboration, "Inclusive Neutral Kaon and Lambda Production in 69 GeV pp Interactions", paper submitted at Conference on New Results from Experiments in High Energy Particle Collisions, Nashville (1973).
5. H. Boggild et al., Nucl. Phys. B27 285 (1971).
6. L. Caneschi and A. Schwimmer, Phys. Letters 33B 577 (1970).
7. G. Neuhoffer et al., Phys. Letters 38B 51 (1972).
8. H. J. Muck et al., "Inclusive Particle Production in pp Interactions at 12 and 24 GeV/c" (Parts I and II), Internal Report DESY-F1-72/1 (1972).
9. For the π^- data see C. M. Bromberg et al., "Study of π^+ and π^- Spectra and Correlations in pp Collisions at 102 GeV/c", to be published.

Table I

Cross Sections for pp → Neutral +n Charged + Anything

n charged	$\sigma(\pi^\circ)$ (mb.)	$\langle n_{\pi^\circ} \rangle$	$\sigma(K^\circ_s)$ (mb.)	$\langle n_{K^\circ_s} \rangle$	$\sigma(\Lambda)$ (mb.)	$\langle n_\Lambda \rangle$
2	7.0 ± 2.6	1.5 ± 0.6	0.36 ± 0.13	0.07 ± 0.03	0.33 ± 0.13	0.07 ± 0.03
4	14.7 ± 3.8	1.9 ± 0.5	0.76 ± 0.18	0.10 ± 0.02	1.15 ± 0.22	0.15 ± 0.03
6	28.0 ± 5.3	3.7 ± 0.7	1.26 ± 0.23	0.17 ± 0.03	0.71 ± 0.17	0.09 ± 0.03
8	14.1 ± 3.8	2.4 ± 0.6	1.02 ± 0.21	0.17 ± 0.03	0.57 ± 0.17	0.09 ± 0.03
10	11.1 ± 3.3	2.9 ± 0.9	0.68 ± 0.18	0.18 ± 0.04	0.41 ± 0.14	0.11 ± 0.04
12	6.2 ± 2.5	3.7 ± 1.5	0.36 ± 0.13	0.21 ± 0.07	0.05 ± 0.05	0.03 ± 0.03
14	1.4 ± 1.2	2.1 ± 1.8	0.04 ± 0.04	0.06 ± 0.06	-	-
16	1.1 ± 1.1	5.0 ± 5.0	0.05 ± 0.05	0.24 ± 0.24	-	-
18	1.5 ± 1.5	27.3 ± 27.3	0.04 ± 0.04	0.77 ± 0.77	-	-
Total	85.0 ± 8.1	2.62 ± 0.25	4.58 ± 0.46	0.141 ± 0.014	3.22 ± 0.37	0.099 ± 0.012

Table II

Transverse Momenta for Particles Produced in pp Collisions at 102 GeV/c.*

Particle	$\langle p_T \rangle$ (GeV/c)	$\langle p_T^2 \rangle$ (GeV/c)^2
γ	0.175 ± 0.020	0.050 ± 0.009
K_s^o	0.424 ± 0.043	0.246 ± 0.038
Λ	0.541 ± 0.060	0.364 ± 0.052
π^-	0.339 ± 0.010	0.171 ± 0.010

* Data are given for $p_T < 1.5$ GeV/c.

Figure Captions

Figure 1 (a) Average number of K°_S (circles) and Λ (crosses) per inelastic pp interaction and (b) average number of π° per inelastic pp interaction as a function of charged multiplicity. The curves are described in the text.

Figure 2 Invariant cross sections

$$F(x) = \frac{2}{\pi\sqrt{s}} \int E \frac{d^2\sigma}{dx dp_T^2} \, dp_T^2$$

as a function of x for (a) $pp \to \gamma x$, (b) $pp \to K^\circ_S x$, and (c) $pp \to \Lambda x$. E, p_L, and p_T are the energy, the longitudinal momentum, and transverse momentum of the particle in the pp center of mass system and $x = 2p_L/\sqrt{s}$. The curves are described in the text.

Figure 3 The cross section $d\sigma/dy$ versus $y = 1/2 \ln [(E + p_L)/(E - p_L)]$ for (a) $pp \to \gamma x$, (b) $pp \to K^\circ_S x$, and (c) $pp \to \Lambda x$.

Figure 4 The cross section $d\sigma/dp_T^2$ versus p_T^2 for (a) $pp \to \gamma x$, (b) $pp \to K^\circ_S x$, and (c) $pp \to \Lambda x$. The p_T^2 distributions have been normalized to account for events from both the forward and the backward hemispheres in the pp c.m. system.

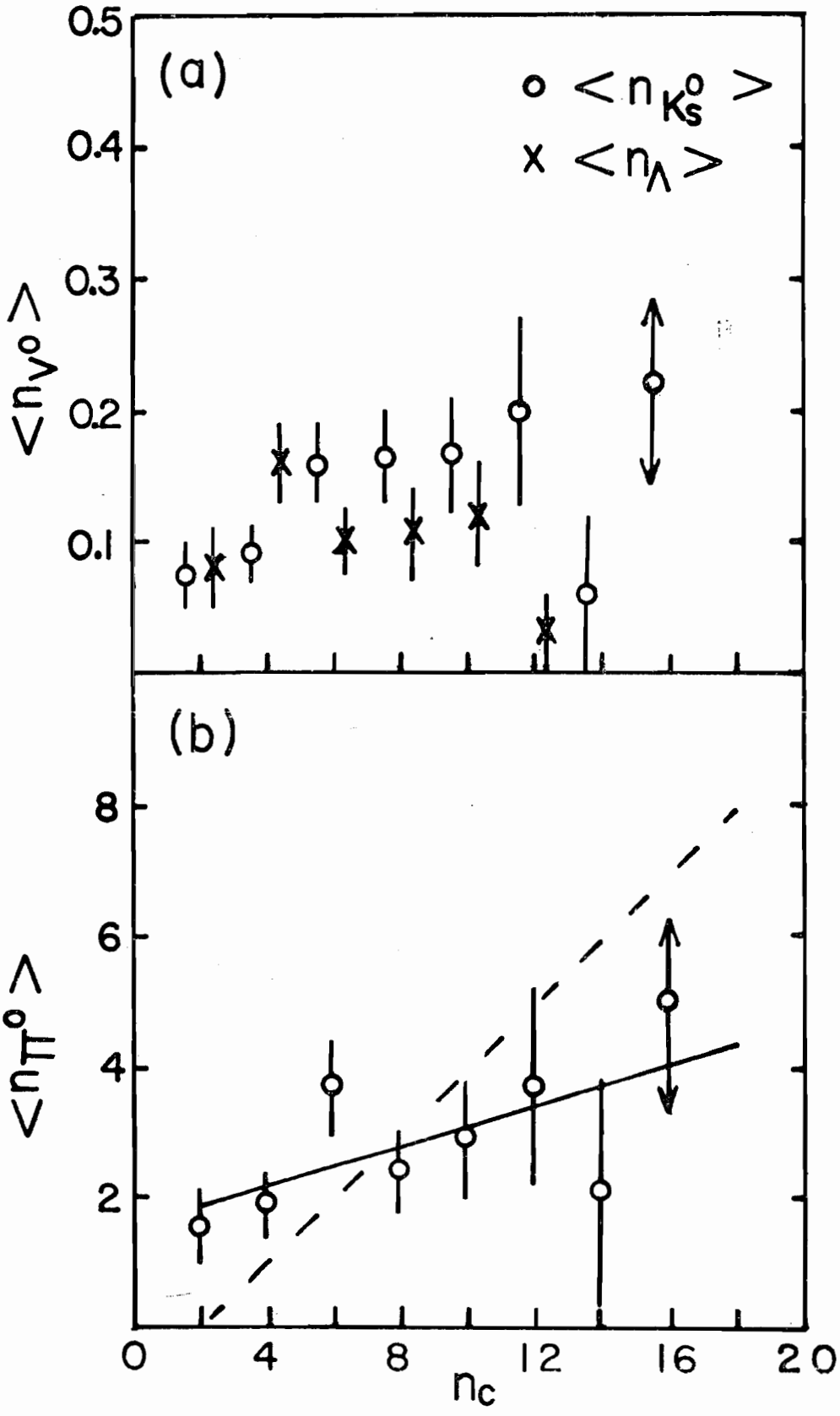
(a)
o $\langle n_{K_S^0} \rangle$
x $\langle n_\Lambda \rangle$
$\langle n_{V^0} \rangle$
0.5
0.4
0.3
0.2
0.1
(b)
$\langle n_{\pi^0} \rangle$
8
6
4
2
0
4
8
12
16
20
n_c

Figure 1

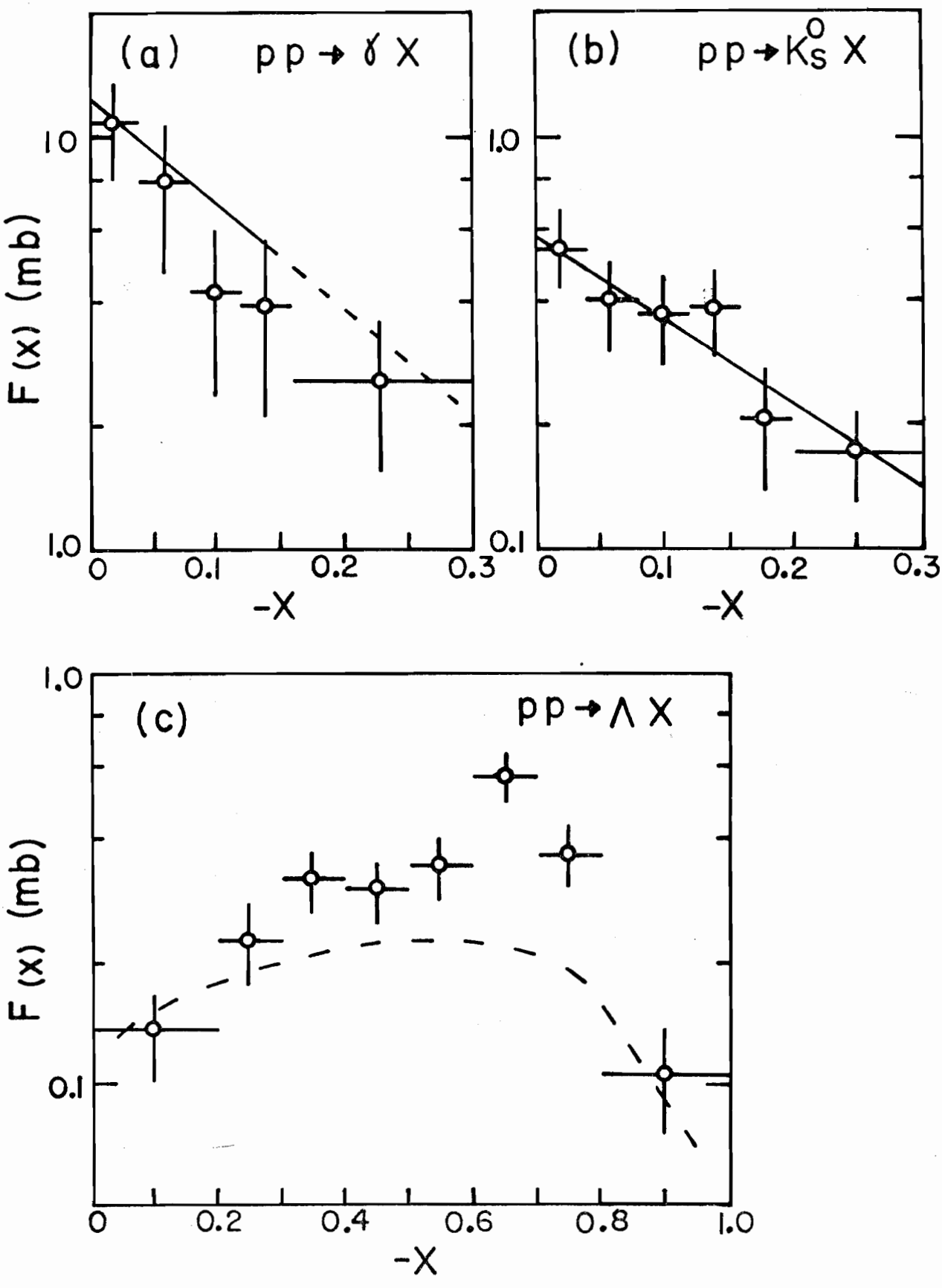

Figure 2

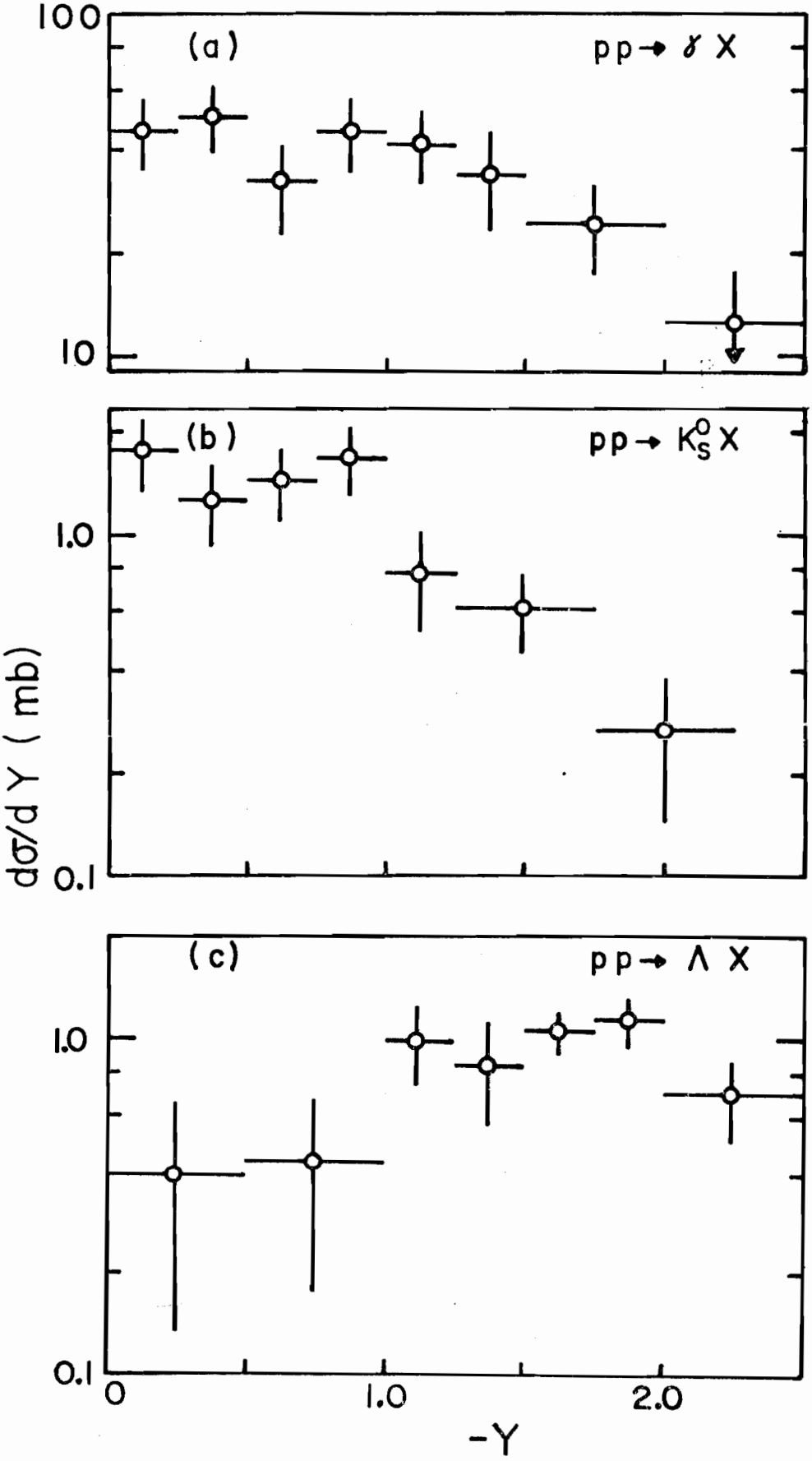

Figure 3

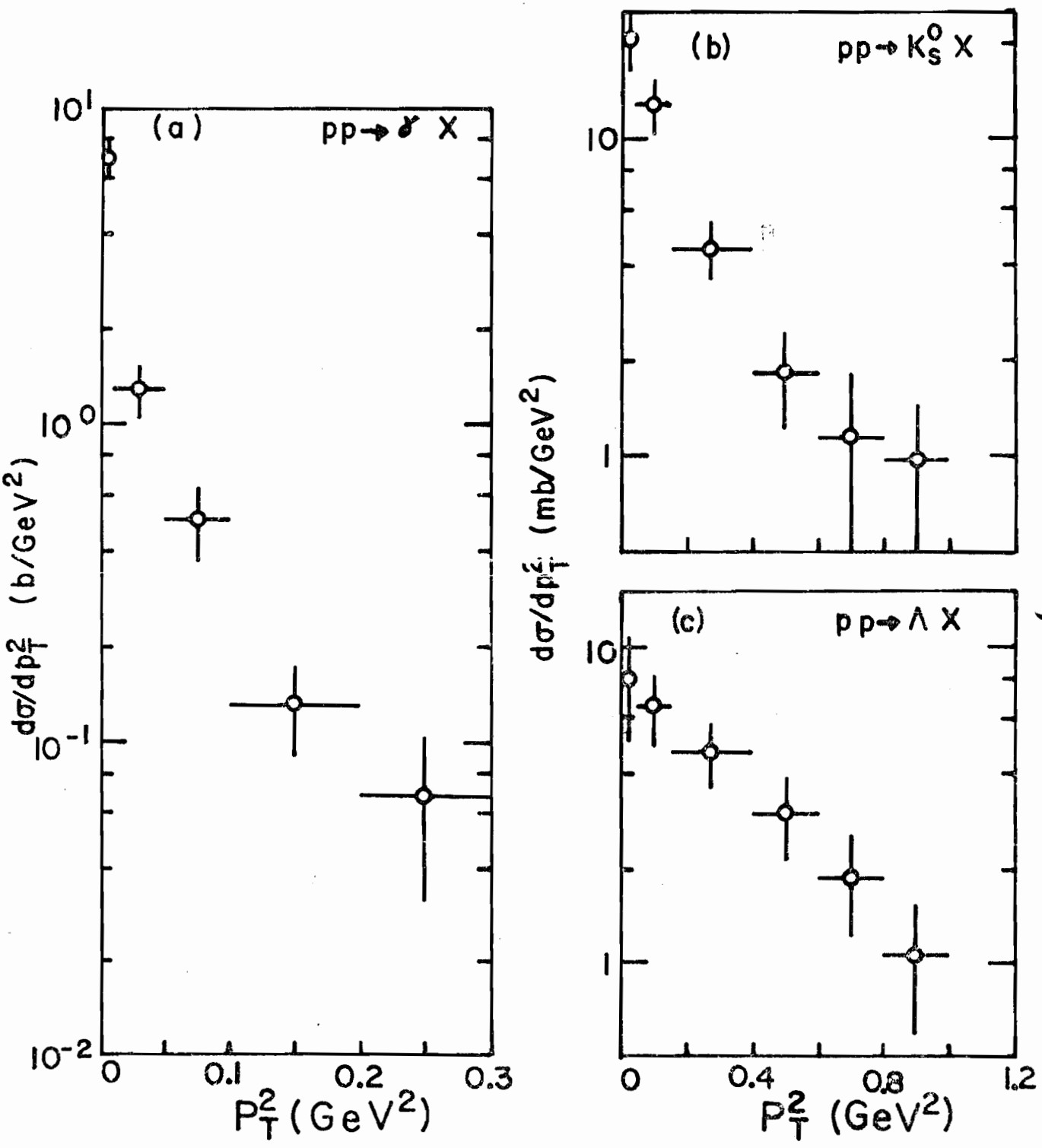
(a)
pp→ γ X
(b)
pp→ K⁰S X
(c)
p p→ Λ X
dσ/dp²T (b/GeV²)
dσ/dp²T (mb/GeV²)
P²T (GeV²)
P²T (GeV²)
10¹
10⁰
10⁻¹
10⁻²
10
1
0
0.1
0.2
0.3
0.4
0.8
1.2

Figure 4